



**RESEARCH PAPER**

**Open Access**



# Estimation of within-gap regeneration height growth in managed temperate deciduous forests using bi-temporal airborne laser scanning data

Louise Leclère<sup>1</sup> , Nicolas Latte<sup>1</sup> , Romain Candaele<sup>1</sup> , Gauthier Ligot<sup>1</sup> and Philippe Lejeune<sup>1\*</sup>

## Abstract

**Key message** Multi-temporal airborne laser scanning (ALS) data were used to estimate regeneration stem height growth within gaps in uneven-aged deciduous forests. The height and height growth measured in the field were used to calibrate and validate ALS estimates. This method provided highly precise estimates of height and unbiased height increment estimates of regeneration at stem level.

**Context** Assessing regeneration height growth is essential for evaluating forest dynamics and optimizing silvicultural operations. However, regeneration description at high spatiotemporal resolution has remained limited to restricted areas by the limiting cost constraints of field measurements. Highly precise airborne laser scanning (ALS) data are currently acquired over wide areas. Such datasets are promising for characterizing regeneration dynamics.

**Aims** We aimed to estimate height and height growth within regenerating areas at the stem level using multi-temporal ALS data.

**Methods** ALS data were acquired from 56,150 ha of uneven-aged deciduous forest in Belgium in 2014 and 2021. Stem tops were detected using local maxima (LM) within regenerating areas in both ALS datasets and matched. Field data were collected in 2021 and used to calibrate the ALS-estimated heights using linear and non-linear models at stem level. Height growth estimation was then validated using field-measured increments.

**Results** Without height calibration, the 2021 ALS-estimated height had a  $-1.06$  m bias and  $1.39$  m root-mean-squared error (RMSE). Likewise, the 2014 ALS-estimated height had a  $-0.58$  m bias and  $1.14$  m RMSE. The non-linear calibration seemed more appropriate for small regeneration stems (height  $< 4$  m). Using height calibration, the 2021 ALS-estimated height had a  $-0.01$  m bias and  $0.84$  m RMSE. In 2014, the bias and RMSE were  $0.02$  and  $0.91$  m, respectively. ALS-estimated height growth was unbiased and had an RMSE of  $0.10$  m-year<sup>-1</sup>.

**Conclusions** This original method is based on the bi-temporal ALS datasets calibrated by limited field measurements. The proposed method is the first to provide unbiased regeneration height growth of regeneration stems in uneven-aged forests and new perspectives for studying and managing forest regeneration.

**Keywords** ALS, LiDAR, Regeneration, Oak-beech forests, Dynamics, Management

Handling editor: John M Lhotka.

\*Correspondence:

Philippe Lejeune  
p.lejeune@uliege.be

Full list of author information is available at the end of the article



© The Author(s) 2024. **Open Access** This article is licensed under a Creative Commons Attribution 4.0 International License, which permits use, sharing, adaptation, distribution and reproduction in any medium or format, as long as you give appropriate credit to the original author(s) and the source, provide a link to the Creative Commons licence, and indicate if changes were made. The images or other third party material in this article are included in the article's Creative Commons licence, unless indicated otherwise in a credit line to the material. If material is not included in the article's Creative Commons licence and your intended use is not permitted by statutory regulation or exceeds the permitted use, you will need to obtain permission directly from the copyright holder. To view a copy of this licence, visit <http://creativecommons.org/licenses/by/4.0/>.

## 1 Introduction

Forests are affected by global changes. Indeed, climate change modifies tree species' growth patterns (Bosela et al. 2021; Martínez del Castillo et al. 2022) and species distribution (Illés et al. 2022). Global changes provoke disease development and pest appearance (Sénécal et al. 2020). Increased wild ungulate density also negatively affects regeneration dynamics (Ramírez et al. 2018; Candaele et al. 2023). These changes necessitate forest monitoring. Assessing the forest regeneration state and its dynamics are necessary to evaluate forest renewal. Regeneration height growth determines these dynamics in the middle term. Evaluating the regeneration development and identifying areas without regeneration are critical to adjust silvicultural operations and ensuring sustainable management.

Field data describing the regeneration state are generally collected at the plot level, as in national forest inventories (Vidal et al. 2016) and forest management inventories (Leclère et al. 2022). However, such inventories usually depend on small plots, their sampling rates are low, and they consider few individuals (Petritan et al. 2009), whereas regeneration is highly spatially heterogeneous. It is therefore difficult to effectively quantify regeneration height growth. In addition, field surveys describing regeneration require extensive organization and are time-consuming and their accuracy is usually limited to cover areas by development stages. Compared with regeneration processes, the spatial and temporal resolution of regeneration data are low due to their aggregation, which limits our understanding of the large-scale regeneration process (i.e., quantifying recruitment). However, such understanding is essential to recognize and manage the impacts of emerging issues, including climate change and ungulate density (Candaele et al. 2023).

Remote sensing data can be used to accurately characterize regeneration. Since 2000, airborne laser scanning (ALS) data has been frequently used to estimate tree and forest attributes, including height, structure, tree species, and biomass (Maltamo et al. 2014). ALS data, which have a high spatial resolution and are acquired over large areas, are promising for overcoming field inventory limitations and are becoming increasingly available. In Nordic countries, where forests are mainly composed of even-aged coniferous stands, forest inventories are primarily based on remotely sensed ALS data (Kangas et al. 2018; Maltamo et al. 2020). ALS data are promising for small and frequent gaps located in deciduous uneven-aged forests that comprise numerous small stems.

To characterize regeneration height growth, it is required to estimate accurately regeneration stem height. ALS underestimates tree height (Holmgren and Nilsson 2003; Heurich et al. 2003; Wang et al. 2019; Michez et al.

2020); indeed, laser pulses do not always reach the top of trees. Tree height is measured on the field from the ground to the top of the tree. For mature trees, height bias is consistent, and ALS-estimated tree height is generally linked to field-measured tree height by a linear relationship (Holmgren and Nilsson 2003; Heurich et al. 2003; Wang et al. 2019; Michez et al. 2020). The height bias (i.e., the origin ordinate of the linear relationship) is approximately 1 m, which creates a challenge when characterizing the height of regeneration stems that are sometimes lower than 1 m. Although some studies have considered a wide range of tree heights (Wang et al. 2019), very few have focused on the characterization of regeneration stem height (i.e., stem height < 10 m).

Characterizing regeneration dynamics by estimating height growth could be investigated using ALS. Previous forest studies that estimated the height growth have mostly focused on mature trees (Hopkinson et al. 2008; Ma et al. 2018; Næsset and Gobakken 2005; Song et al. 2016; Vepakomma et al. 2008, 2011; Yu et al. 2004, 2006; Zhao et al. 2018). Tree height growth has mainly been studied in boreal and temperate forests over rather small forest areas (26–3225 ha), considering mature plantations and regular stands of coniferous species. At least two ALS datasets are required to study height growth; however, additional datasets can also be used (Hopkinson et al. 2008; Song et al. 2016; Zhao et al. 2018). A sufficient temporal gap between ALS acquisitions is also required (Næsset and Gobakken 2005; Yu et al. 2004). Previous studies have considered at least five growing seasons (Hopkinson et al. 2008; Vepakomma et al. 2011; Ma et al. 2018; Song et al. 2016). In general, ALS datasets have different acquisition dates (leaf-on/off), sensors, flight configurations, and point densities within and between studies (Table 1). These characteristic differences between the ALS point clouds can complicate height growth estimation.

Both plot and tree level height growth studies have been published. At the tree level, tree crowns were detected automatically (Ma et al. 2018; Song et al. 2016; Vepakomma et al. 2008, 2011; Yu et al. 2006; Zhao et al. 2018) or digitized manually (Yu et al. 2004). Height growth was then estimated for each tree, considering height variations within crowns or in a buffer zone around the tree tops (Vepakomma et al. 2011). However, height growth estimates at the tree level were not validated in some studies (Vepakomma et al. 2008, 2011), whereas other studies partially validated the estimates by comparing height growth to tree heights and basal areas or diameter at breast height (DBH) variations measured in the field (Ma et al. 2018; Song et al. 2016). Some studies completely validated their results using field measurements of height growth (Yu et al. 2004, 2006; Zhao

**Table 1** Airborne laser scanning (ALS) datasets and acquisition parameters used in previous studies

	Yu et al. (2004)	Yu et al. (2006)	Hopkinson et al. (2008)	Vepakomma et al. (2008)	Vepakomma et al. (2010)	Song et al. (2016)	Næsset and Gobakken (2005)	Ma et al. (2018)
<b>Sensor</b>	TopoSys-1	Toposys-1 Toposys-2	ALTM sensor 1225 to 3100	ALTM1020 ALTM 2050 ALTM 3100	ALTM 1020 ALTM 2050	ALTM2050 Riegl LMS-Q560	ALTM 1210	Optech GEMINI
<b>Dates</b>	Sept. 1988 June 2000	Sept. 1988 May 2003	Sept 2000 July 2002 Nov. 2004 Dec. 2005	June 1998 Aug. 2003 July 2007	June 1998 Aug. 2003	Oct. 2004 Aug. 2008 Aug. 2010	June 1999 July 2001	2007–2008 2012–2013
<b>Altitude (m)</b>	400	400	800 to 1000	700 to 1000	700 1000	1000 300	700 850	600–800
<b>Laser pulse frequency (kHz)</b>	83	83	25 to 50	5 50 67	4 50	50 150	10 10	100
<b>Scan frequency (Hz)</b>	/	653	30 to 44	/	/	67 80	21 30	40–60
<b>Scan angle (°)</b>	±7.1	±7.1	±12 to ±18	/	±10 ±15	±5.3 ±30	±17 ±16	±12–±14
<b>Density</b>	10 pulses/m <sup>2</sup>	10 pulses/m <sup>2</sup>	2.5 to 3.6 returns/m <sup>2</sup>	0.33 to 10 hits/ m <sup>2</sup>	0.3 3 hits/m <sup>2</sup>	11.3 51.8 returns/m <sup>2</sup>	1.18 0.87 pulses/m <sup>2</sup>	10 points/m <sup>2</sup>

et al. 2018). At the plot level, tree height growth was estimated using changes in height distribution (Hopkinson et al. 2008), canopy height model (CHM) differences (Song et al. 2016), regression analysis (Næsset and Gobakken 2005), or aggregated tree level estimates (Yu et al. 2004). Height growth estimates were partially validated by comparing the changes in field-measured heights and basal area growth (Song et al. 2016) or comparing the plot-level estimates of height growth distribution to plot-level height growth distribution measured in the field (Hopkinson et al. 2008). Height growth at the plot level were also completely validated using field measurements (Næsset and Gobakken 2005; Yu et al. 2004). In addition, some studies have evaluated the influences of factors on tree height growth, including canopy opening, topography, competition, forest structure, and species type (Ma et al. 2018; Næsset and Gobakken 2005; Vepakomma et al. 2008). However, few studies have focused on estimating regeneration height growth.

This study aimed to characterize large-scale (561.50 km<sup>2</sup>) regeneration height and height growth at the stem level, including small regeneration stems (i.e., below the inventory threshold, fixed at a 40 cm circumference in Belgium), using bi-temporal ALS data (7–8 growing seasons). The method was developed for a managed-temperate uneven-aged deciduous forest, which is challenging for such investigations. This study was developed to answer the following questions:

- Is the relationship, between the ALS-estimated height and field-measured height, linear as for mature

trees? Will a non-linear model be more appropriate for estimating the height of regeneration stems?

- How can multi-temporal ALS data be used to estimate regeneration height growth at the stem level within regenerating areas? And with what accuracy?

## 2 Materials and methods

### 2.1 Study area

The study area was located in Wallonia (southern Belgium). The selected forests comprised 56,150 ha of uneven-aged deciduous forest with similar management practices (Fig. 1) and the two main species beech (*Fagus sylvatica* L.) and oak (*Quercus robur* L. and *Quercus petraea* (Mattuschka) Liebl) (Alderweireld et al. 2015). The selected forests contained at least 30% beech trees (Bolyn et al. 2022) and are primarily managed using continuous cover forestry (Pommerening and Murphy 2004) that involves the creation of small gaps to initiate regeneration growth. The regeneration therefore expands per dense groups. The elevation above sea level in the study area ranged from 128 to 591 m, with occasionally hilly topography (mean slope = 7.5° ± 6.7°) and a temperate continental climate (<https://www.eea.europa.eu/>) characterized by a mean annual rainfall of 1158 mm and a mean annual temperature of 8.99 °C.

According to common management practices in the region, regeneration was defined as stems with a circumference, measured at 1.5 m height, below 40 cm (i.e., seedlings to established saplings). The regeneration mainly developed in beech trees, as oak regenerated minimally within the study area (Alderweireld et al. 2015).

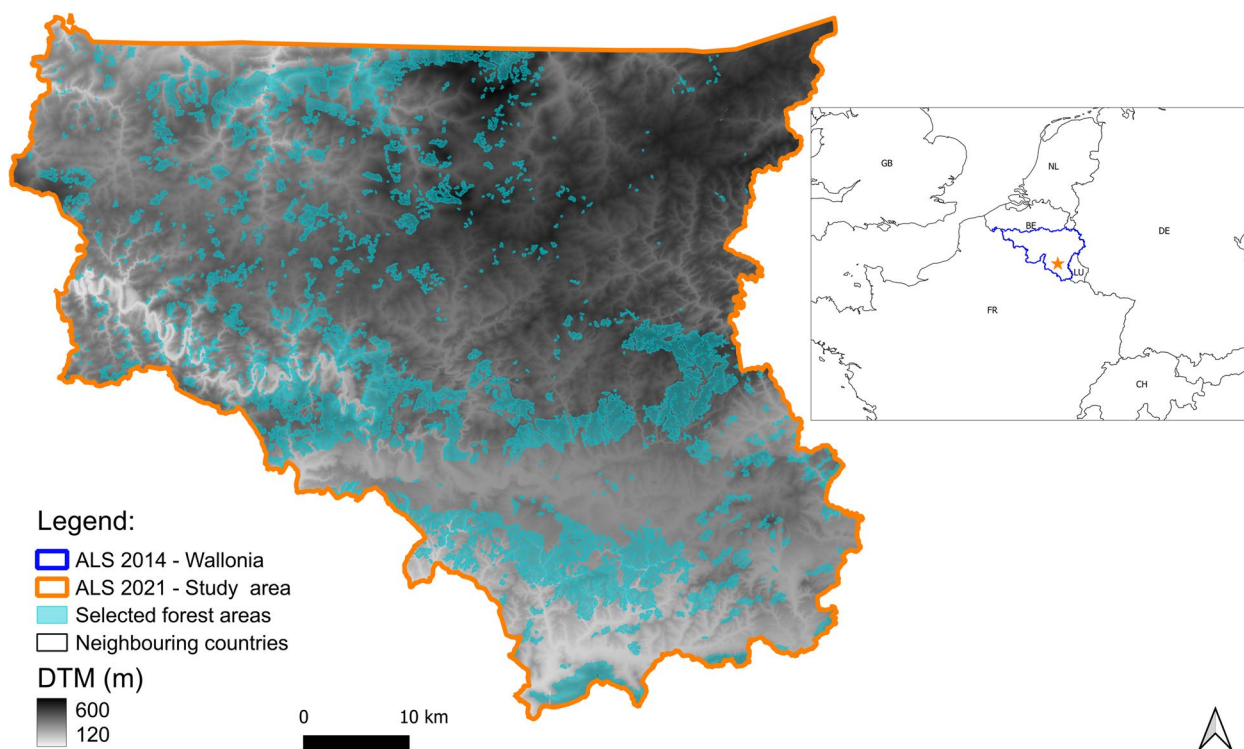


**Fig. 1** Study area. The 2014 and 2021 airborne laser scanning acquisition areas are indicated in blue and orange, respectively. The studied forest areas are shown in light blue. DTM, digital terrain model; LU, Luxembourg; FR, France; GE, Germany; NL, Netherlands; CH, Switzerland; GB, Great Britain

### 2.2 ALS data

A multi-temporal method was developed using two ALS datasets (Table 2). The first discrete-return ALS data were acquired in March–April 2013 and February–March 2014 using a Riegl Litemapper 6800i sensor under leaf-off conditions (called “2014 ALS” thereafter). The second dataset was acquired in February–March 2021 using a Riegl LMS-Q780 sensor under leaf-off conditions. The time delay between the LiDAR acquisitions was 7–8 growing seasons.

ALS data were processed using the *LidR* package (Roussel et al. 2020). The ALS point clouds were

normalized (using the *tin* algorithm) based on the ground classification. A CHM was built for each normalized point cloud with a spatial resolution of 1 m using the *pit-free* method implemented using many thresholds (Khosravipour et al. 2014). Both ALS point clouds were treated using the same functions and parameters. ALS acquisition was performed to produce homogeneous CHMs with the same resolution.

The ALS datasets differed with respect to the sensor model and configuration, acquisition dates, flight parameters, point cloud properties, and georeferencing. Owing to these differences, the forest canopy details differed for

**Table 2** Sensor and ALS point cloud properties

Property	2014 ALS	2021 ALS
Sensor	Riegl Litemapper 6800i	Riegl LMS-Q780
Platform	Plane	Plane
Acquisition date	March–April 2013 February–March 2014	February–March 2021
Number of returns recorded per pulse	Up to 4	Up to 7
Pulse frequency (kHz)	150	400
Scan angle (°)	± 60	± 28
Mean point density (pts/m <sup>2</sup> )	3	13

both CHMs (Fig. 2A, B). A simple algebraic difference could not be performed without further precautions to estimate regeneration height growth (Fig. 2C). This issue was more complicated for regeneration stems.

### 2.3 Method workflow

The proposed method was developed to estimate the regeneration height growth at the stem level (Fig. 3). A field dataset was collected to calibrate the ALS heights for both datasets and to validate the ALS height growth. The calibration procedure compared linear and non-linear models. To study regeneration on a large scale, height growth was estimated for the local maxima (LM) detected within the regenerating areas in the selected forests. Data processing was implemented using *R* (R core team 2020).

### 2.4 Detection of regenerating areas

Regeneration height growth was studied within regenerating areas of the selected forests (Fig. 3). In the proposed method, regenerating areas corresponded to gaps that closed from below owing to regeneration growth. Regenerating areas are forest areas not overtopped by dominant trees; therefore, they contain seedlings and saplings expected to thrive, some of which are expected to become recruited trees. Gaps in 2014 were delineated on the CHM using a thresholding method that considered a maximum vegetation height of 10 m, minimum surface area of 50 m<sup>2</sup>, and minimum width of 4 m, as described by Leclère et al. (2021). Regenerating areas were defined as areas that were gaps in 2014 with vegetation heights ≥ 50 cm (considered to be established regeneration). A height difference between 2014 and 2021 of < 7 m, which was calculated using both CHMs, was added to exclude areas corresponding to the lateral

growth of tree crowns at the edges of regenerating areas (i.e., gaps closing from above). The 7 m threshold was fixed based on field observations. Regenerating areas below 20 m<sup>2</sup> were removed as they were too small for optimal regeneration growth due to lack of space and light. Regenerating areas greater than 2000 m<sup>2</sup> were also removed as they were border artifacts or plantations.

### 2.5 Stem top position

To analyze regeneration heights and height growth at the stem level, stem top positions were detected automatically within the regenerating areas using LM (Fig. 3). Thus, the LM corresponded to the dominant stems within the regenerating areas. LM detection was performed on the 2021 and 2014 CHMs within regenerating areas using the *lmf* algorithm (Popescu and Wynne 2004) of the *lidR* package. The size of the moving window varied according to the canopy height. The window diameter was fixed using Eq. 1 based on previously published data and field observations. The detection height threshold was set at 2 m for 2021 and 0.50 m for 2014.

$$\text{Window diameter} = \text{height} \times 0.15 + 2.2 \quad (1)$$

### 2.6 LM matching

The LM detected on the 2021 and 2014 CHMs were matched (Fig. 3). The matching procedure was implemented for each regenerating area. The 2021 and 2014 ALS heights were extracted from the CHMs at the LM positions (i.e., the stem top positions). Thus, the 2021 ALS height ( $H_{21}$ ) was defined as the 2021 CHM value at the 2021 LM position, while the 2014 ALS height ( $H_{14}$ ) were defined as the 2014 CHM value at the 2014 LM position. The 2021 LM were sorted by decreasing height. Starting with the highest 2021 LM, matching was

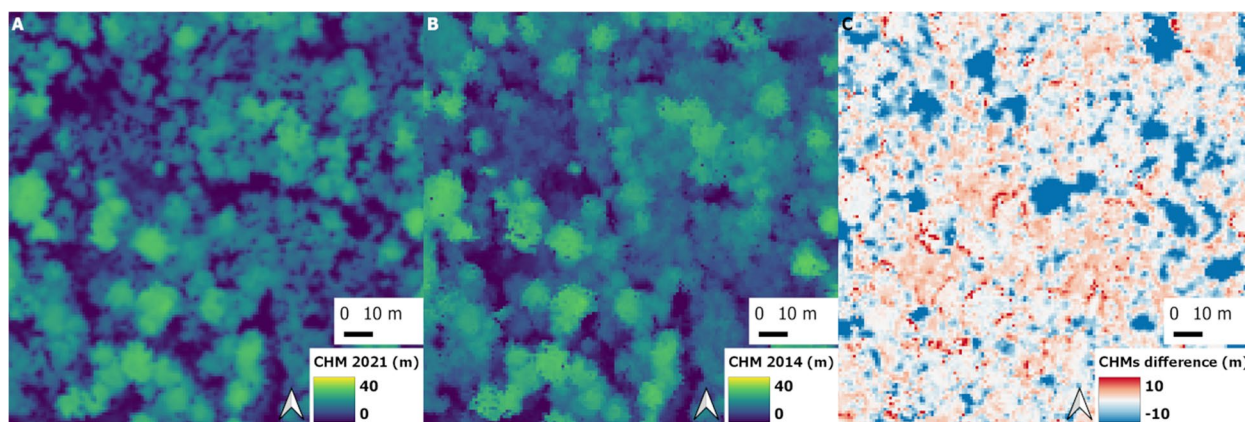


**Fig. 2** Canopy height models (CHMs) and their differences at the same field location. **A** CHM 2021 raster. **B** CHM 2014 raster. **C** CHM difference raster. Dark red pixels correspond to high positive height differences induced by the lateral growth of tree crowns at gap edges, whereas light red pixels correspond to regeneration height growth. Dark blue pixels denote high negative height differences because of harvested trees

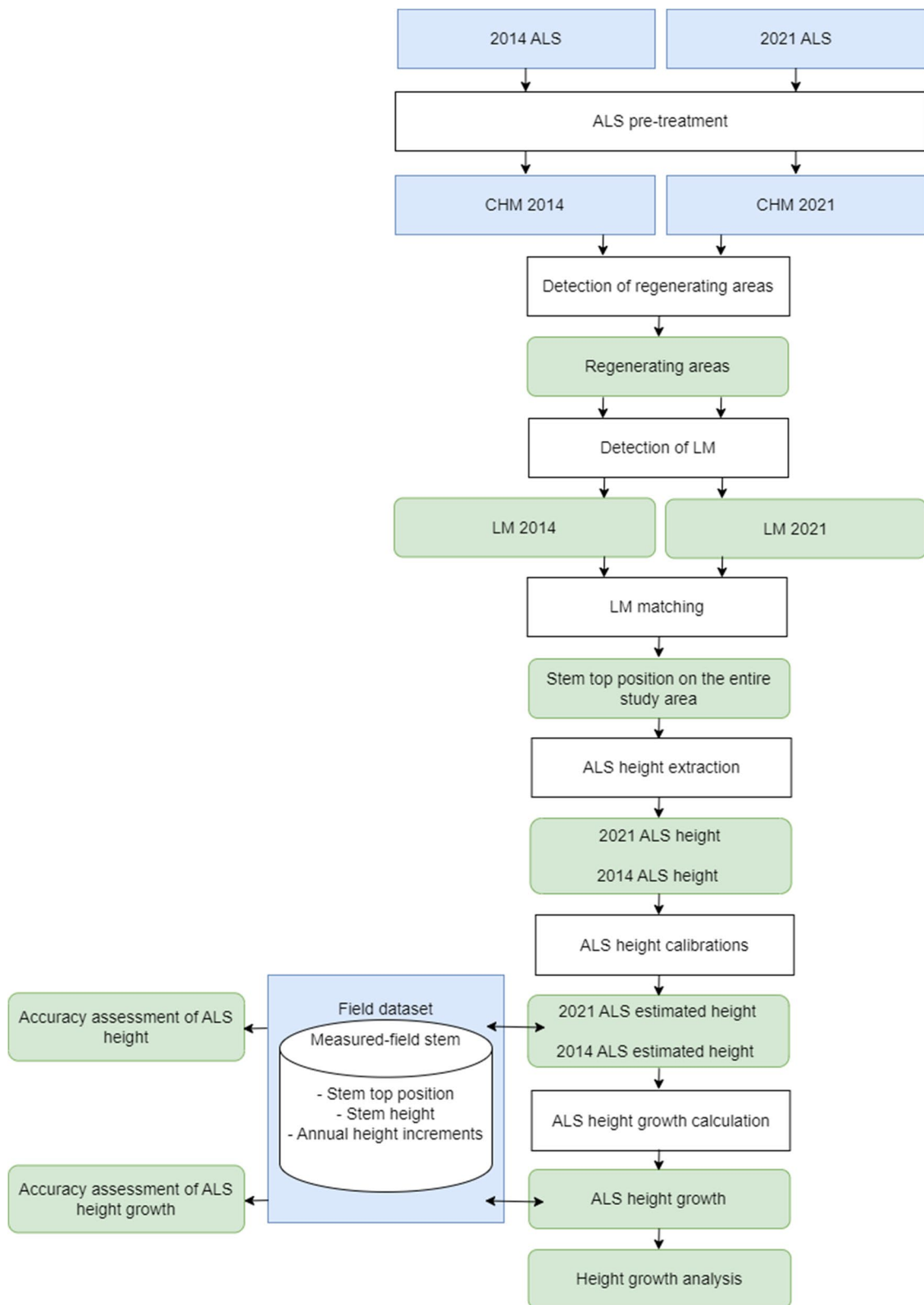


**Fig. 3** Method workflow used in this study

performed by considering the closest 2014 LM (planar distance) not yet assigned in a maximum distance buffer. The maximum distance buffer was set to the radius of the moving window used to detect the LM (Eq. 1).

### 2.7 Reference dataset

A field reference dataset (Fig. 3) was acquired to calibrate the ALS heights from 2014 and 2021, as well as to validate height growth at the stem level. A field survey was conducted between March and November of 2022 to measure the height and height increments of selected stems. Height increments were derived from budding scars on the main stem (Yu et al. 2006; Zhao et al. 2018). In some deciduous species, such as beech, the terminal bud leaves a budding scar on the stem each year following development (Fig. 4A) (Thiébaud et al. 1992). Therefore, the annual height increment (i.e., the distance between two scars) can be measured by identifying successive budding scars on the beech stem (Fig. 4B).

Beech trees occasionally produce a second shoot (Teissier du Cros 1981); however, multiple shoot elongations are less common in natural regeneration (Kiss and Claessens 2002) and secondary shoots are easily identifiable by finer scars and different leaf arrangements (Dupré et al. 1985). Therefore, stem analysis is reliable for identifying annual increases in beech height.

A total of 123 stems were selected from 60 regenerating areas to measure the height increments. The selected

stems were dominant in the regenerating areas, which covered the altitude gradient (345–540 m) and the 2021 height range. These stems corresponded to beech with heights of 3–16 m. Stems were cut down, after which scars left each year on the stem by the terminal buds were identified from the apex (Fig. 4A). The annual height increments in 2014–2021 were then measured (Fig. 4B, C) and the corresponding average height growth (called “field-measured height growth” thereafter) was estimated for each stem. A stem disc was collected from each stem to verify whether the number of rings corresponded to the number of measured increments. The stem disc was collected behind the last identified budding scar. The 2021 stem heights were also measured in the field (2021 field-measured height), and the stem tops were geolocated using an Emlid Reach RS2+GPS (Emlid, <https://emlid.com/reachrs2plus/>). In addition, the 2014 field-measured heights were determined for each stem by subtracting the total 2014–2021 height increments from the 2021 field-measured heights. Each stem was assigned to a matched pair of LMs using photo interpretation, which was called the reference dataset.

### 2.8 ALS height calibrations

To estimate regeneration height growth, the 2021 and 2014 ALS heights were calibrated using the reference dataset (Fig. 3). Indeed, ALS underestimates tree height because laser impulsion does not always reach the top

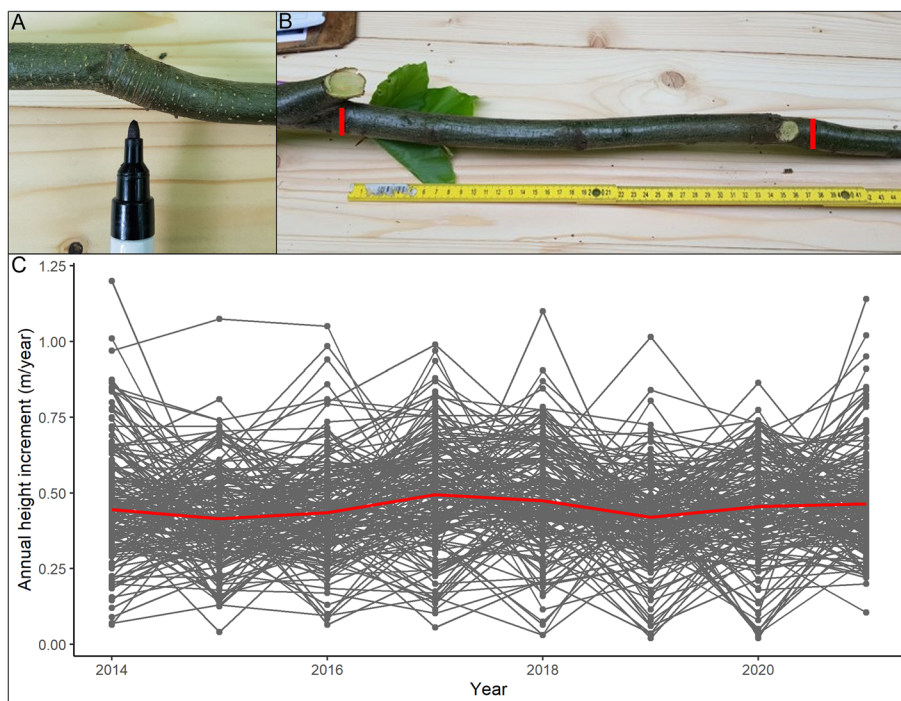


**Fig. 4** Height growth field measurements. **A** Identification of scars left on the stem by terminal buds. **B** Measurement of an annual increment. **C** Measured annual height increments per year at the stem level and median annual heights (red line)

of trees. The tree height estimation bias depends on the point cloud density (Zhao et al. 2018). The 2021 and 2014 ALS heights were calibrated to correct the height bias, as described by Zhao et al. (2018). First, linear models (Eqs. 2 and 3) were used for the ALS height calibration:

$$H_{Est21\_Lin} = b_{21} + a_{21} \times H_{21} \tag{2}$$

$$H_{Est14\_Lin} = b_{14} + a_{14} \times H_{14} \tag{3}$$

where  $H_{21}$  is the 2021 ALS height;  $H_{Est21\_Lin}$  is the 2021 ALS-estimated height using the linear model;  $H_{14}$  is the 2014 ALS height;  $H_{Est14\_Lin}$  is the 2014 ALS-estimated height using the linear model;  $b_{21}$ ,  $b_{14}$ ,  $a_{21}$ , and  $a_{14}$  are the model parameters. Equations 2 and 3 were adjusted for the reference dataset at the stem level using the *lm* function in the *stats* R package (R Core Team 2020). Residuals were checked; the bias (i.e., mean residuals) and root-mean-squared error (RMSE) were estimated.

However, linear models (Eqs. 2 and 3) are not appropriate for estimating the height of regeneration stems. Indeed, the height of regeneration stems could be below  $b_{21}$  and  $b_{14}$  parameters. A non-linear curve-like model (Eq. 4), using a generalized additive model (GAM), was thus tested for the ALS height calibration:

$$H_{Est\_GAM} = s(H_{ALS}) + s(H_{ALS} * year) \tag{4}$$

where  $H_{ALS}$  is the 2021 and 2014 ALS height; *year* is the ALS acquisition year (considered as a factor value);  $H_{Est\_GAM}$  is the 2014 or 2021 ALS-estimated height using the GAM.

Equation 4 was adjusted for the reference dataset at the stem level using the *gam* function in the *mgcv* R package (Wood 2017). The parameter *k* was set to 3 and the *scat()* function was used as family option. Residuals were checked and the bias and RMSE were estimated.

The 2021 and 2014 ALS heights were estimated using calibration models for all LM within the study area.

### 2.9 ALS height growth estimation

The ALS height growth (m·year<sup>-1</sup>) was estimated (Fig. 3) using Eqs. 5 and 6:

$$ALS\ height\ growth_{Lin} = \frac{H_{Est21\_Lin} - H_{Est14\_Lin}}{nGrowingSeasons} \tag{5}$$

$$ALS\ height\ growth_{GAM} = \frac{H_{Est21\_GAM} - H_{Est14\_GAM}}{nGrowingSeasons} \tag{6}$$

where *nGrowingSeasons* is the number of growing seasons that elapsed between the ALS acquisitions. The stem-level reference dataset was used to assess the ALS height growth estimations. The ALS and field-measured

height growth were then compared graphically, and the bias and RMSE were calculated.

ALS height growth was estimated for each LM located within the study area. LMs with positive height increment were retained for further analysis. Negative height increment was observed owing to broken branches in the stem crowns or stems becoming leaner (Vepakomma et al. 2011; Yu et al. 2004).

## 3 Results

### 3.1 ALS-estimated heights

The 2021 and 2014 ALS heights were calibrated using the field-measured heights based on linear and GAM models (Figs. 5 and 6). Without calibration, 2021 field-measured height was estimated with a bias of -1.06 m and a RMSE of 1.39 m (Fig. 6A). The 2014 field-measured height was estimated with a bias of -0.58 m and a RMSE of 1.14 m without calibration (Fig. 6D).

ALS height calibration was first carried out using linear models (Fig. 5). The parameters used for Eqs. 2 and 3 are listed in Table 3. After the 2021 ALS linear calibration, bias and RMSE were 0.00 m and 0.87 m, respectively (Fig. 6B). In addition, after the 2014 ALS linear calibration, bias and RMSE were 0.00 and 0.95 m, respectively (Fig. 6E).

The ALS height calibration was secondly carried out using a GAM (Fig. 5). The parameters used for Eq. 4 are listed in Table 4. After the 2021 ALS GAM calibration, bias and RMSE were -0.01 and 0.84 m, respectively (Fig. 6C). In the same way, after the 2014 ALS GAM calibration, bias and RMSE were 0.02 and 0.91 m, respectively (Fig. 6F). Figure 7 presents the ALS height residuals according to the field-measured height for the three studied case (without calibration, linear calibration, and GAM calibration). The GAM improved the height calibration of small stems (considered as 2014 height ≤ 3 m and 2021 height ≤ 5 m) (Figs. 5, 7). Using the GAM height calibration, the average residual height value of small stems was 0.52 m for the 2021 ALS dataset and 0.50 for the 2014 ALS dataset. When using the linear models, these values were equal to 0.85 and 0.65 m, respectively.

### 3.2 ALS height growth accuracy

Without the height calibration, height growth of the regeneration stems was estimated with a bias of -0.07 m·year<sup>-1</sup> and a RMSE of 0.13 m·year<sup>-1</sup> (Fig. 8A). Both height calibrations improved ALS height growth estimation of regeneration stems. Conversely, after linear height calibration, stem height growth was estimated with a bias of 0.00 m·year<sup>-1</sup> and a RMSE of 0.10 m·year<sup>-1</sup> (Fig. 8B). Using GAM height calibration, stem height growth was estimated with a bias of -0.01 m·year<sup>-1</sup> and



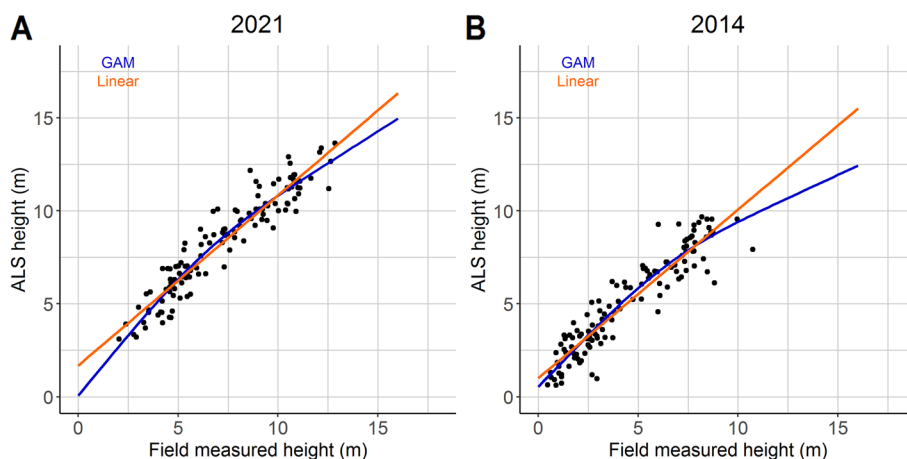


**Fig. 5** ALS height according to field-measured height of regeneration stems with their fitted linear and GAM relations for the years 2014 and 2021. **A** 2021 ALS dataset. **B** 2014 ALS dataset

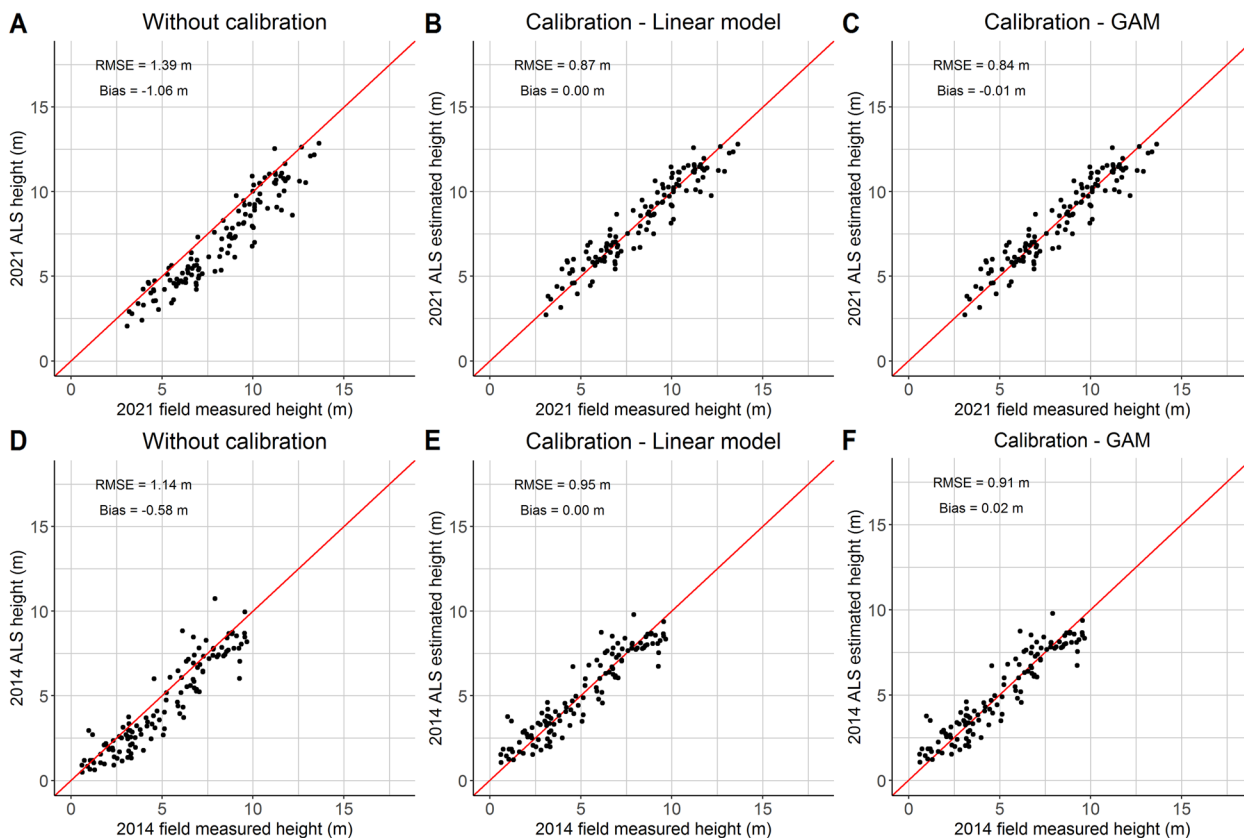


**Fig. 6** Goodness of fit of the calibrated ALS height according to field-measured height. **A, D** Raw data (without calibration). **B, E** Linear-calibrated. **C, F** GAM-calibrated. Results are presented for the 2021 ALS (**A–C**) and the 2014 ALS (**D–F**) datasets

a RMSE of 0.10 m·year<sup>-1</sup> (Fig. 8C). Figure 9 shows the height growth residuals according to the 2021 field-measured height for the three studied case (without calibration, linear calibration, and GAM calibration).

### 3.3 Analysis of ALS height growth in the study area

In total, 268,983 stems (LM pairs) were detected within the selected forests in the study area (Fig. 10), for which the ALS height growth was 0.00–1.07 m·year<sup>-1</sup>. The

**Table 3** 2021 and 2014 height model parameters

Year	Parameter	Estimate	Standard error	tvalue	Significance	R <sup>2</sup>
2021	b <sub>21</sub>	1.67	0.23	7.38	2.28e−11 (***)	0.89
	a <sub>21</sub>	0.92	0.02	31.35	<2e−16 (***)	
2014	b <sub>14</sub>	1.00	0.17	5.83	4.71e−08 (***)	0.86
	a <sub>14</sub>	0.91	0.03	27.73	<2e−16 (***)	

\*\*\* =“very highly significant”

mean ALS height growth was 0.45 (±0.17) m·year<sup>−1</sup>, and the height growth at the stem level exhibited a generally normal distribution (Fig. 11). The detected stems were located in 84,528 regenerating areas. The regenerating areas ranged from 21 to 1959 m<sup>2</sup> in size, with a mean measured area of 175 (±195) m<sup>2</sup>. The total regenerating area covered 1474.7 ha, corresponding to 2.62% of the deciduous forests of the study area. The number of stems detected in the regenerating areas ranged from 1 to 68, with a mean of 3.16 (±4.02) stems.

In 2021, the stems had heights ranging from 2.65 to 17.07 m, with a mean height of 10.09 m (±2.30 m). In 2014, the stem height was 1.10–10.00 m, with a mean height of 6.95 m (±2.34 m)

## 4 Discussion

### 4.1 Height and height growth estimates

In this study, we proposed a method for stem-level estimation of regeneration height and height growth over a large area based on ALS dataset comparisons with individual stem identification using the LM approach. The novelty of this method is that two ALS datasets acquired in different years (2014 and 2021) were height calibrated based on minimal field measurements collected during a unique field survey (date 2021). This study combines the precision of field measures with the wide spatial coverage of ALS datasets. The calibration increased the precision and robustness of the stem height estimations and required minimal field measures. The GAM calibration improved the

ALS-estimated height for small regeneration stems (height < 4 m) and overall robustness in comparison to linear calibration. The developed method produced unbiased stem level height growth estimates. This is a considerable advantage over field data collection for estimating height growth over large areas.

ALS bias correction based on field measurements improves the handling of the ALS dataset characteristics (i.e., point cloud properties and georeferencing accuracy) and acquisition parameters (i.e., sensors, acquisition configuration, dates, and flight parameters), which may influence stem height estimates. Although correction methods based on the ALS data characteristics and without field measurement requirements have been proposed, these methods do not address several bi-temporal ALS stem growth estimation issues. Depending on the stem crown size and ALS point cloud density, the tree-tops are not usually reached (Wang et al. 2019), and stem conformation may evolve during ALS data acquisition (e.g., loss of branches, straightening of a leaning tree, or tree leaning) (Song et al. 2016). Owing to these challenges, estimating parameters such as tree height is sometimes erroneous between datasets (Roussel et al. 2017). Consequently, the method proposed herein produced unbiased estimates with slightly better goodness of fit (RMSE=0.10 m) than previous tree-level height growth estimates obtained for mature deciduous and boreal forests (Yu et al. 2006; Zhao et al. 2018). Obtaining such precision at the stem level is crucial, considering the technical challenges associated with regeneration characterization. Field data are also required, necessitating particular precautions. The crowns of the selected stems must be identified and geolocated correctly. However, we assume that these measurements are valuable regarding their limited costs. Future studies should establish the relationship between calibration data and quality.

### 4.2 Height growth analysis across the 56,150 ha of the study area

The method developed in this study allowed us to estimate the regeneration height growth over a wide area using multi-temporal ALS data. The mean stem regeneration height growth obtained using this method was

**Table 4** Generalized additive model (GAM) parametric coefficients and significance of the smoothing terms

Parametric coefficients				
Factor	Estimate	Standard error	t value	Pr (> t )
Intercept	6.58	0.33	19.9	<2e−16 (***)
Approximate significance of smoothing terms				
Smoothing term	Edf	Ref.df	Chi.sq	p value
s(H_ALS)	1.95	2.00	105.79	<2e−16 (***)
s(H_ALS*year)	1.87	4.00	37.88	<2e−16 (***)

\*\*\* =“very highly significant”

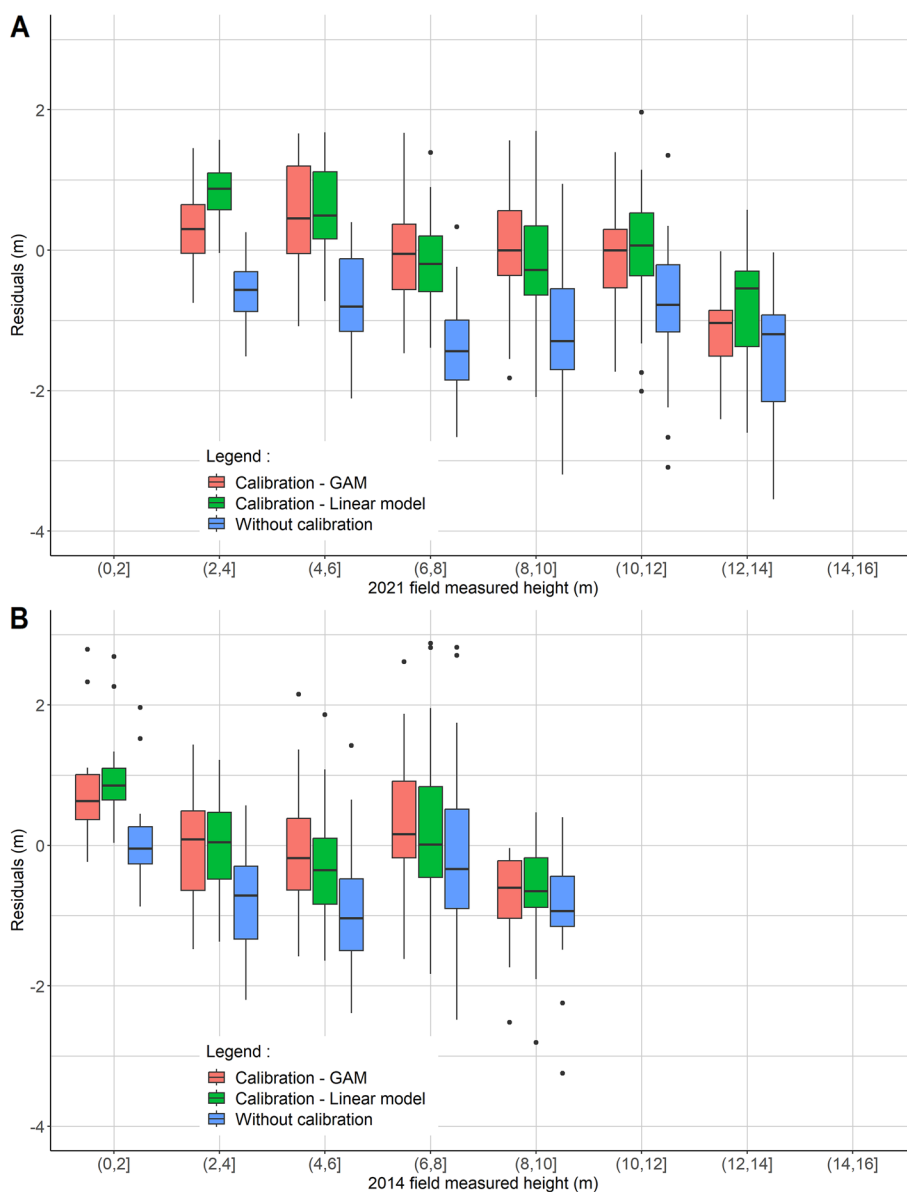


**Fig. 7** ALS height residuals according to field-measured height for the three calibrations (raw data, linear-calibrated, and GAM-calibrated). **A** 2021 ALS dataset. **B** 2014 ALS dataset. Height residual was calculated as ALS height – field-measured height

0.45 m·year<sup>-1</sup> (±0.17) (Fig. 11), and the variations in the height growth estimates were small. The proposed method did not consider the stem species, but the values and variations of the estimates are consistent with in situ studies of oak–beech regeneration (<3 m) in the Ardenne bioclimatic region (Ligot et al. 2013). Beech accommodates various climatic and trophic conditions when hygrometry is high and precipitation is constant (Teissier du Cros 1981). In addition, beech height growth rapidly plateaus as the percentage of above-canopy light increases (Ligot et al. 2013; Stancioiu and O’ Hara 2006), which explains its low height growth variability compared with

other species, such as Norway spruce, silver fir, maple, and ash (Petritan et al. 2009; Stancioiu and O’ Hara 2006). In this study, we focused our growth observations on the gaps; therefore, the light supply for regeneration height growth was not a limiting factor for the dominant regeneration stems (Feldmann et al. 2020; Noyer et al. 2019).

### 4.3 Perspectives for forest management and regeneration-related studies

The method developed herein has considerable implications for forest management, which requires exhaustive

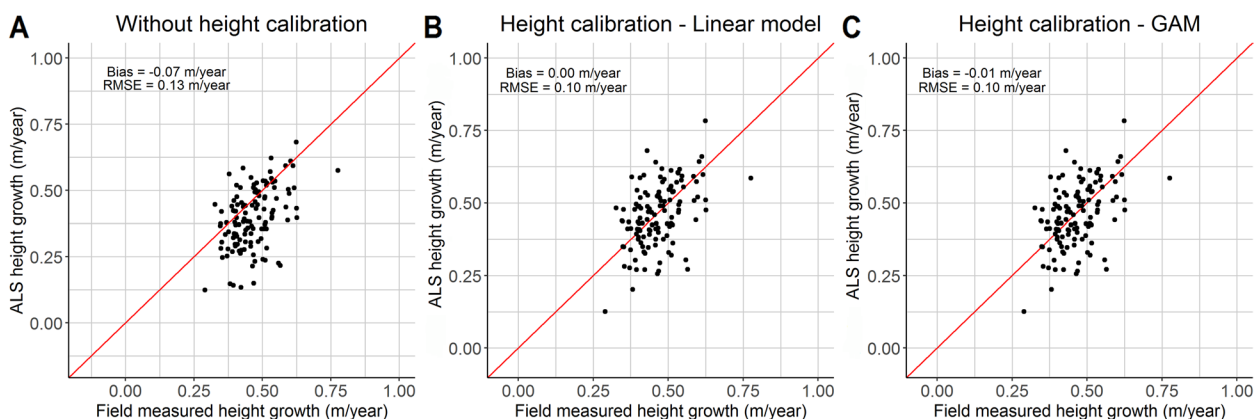


**Fig. 8** ALS height growth according to field-measured height growth of regeneration stems. **A** ALS height growth without height calibration. **B** ALS height growth with linear height calibration. **C** ALS height growth with height GAM calibration

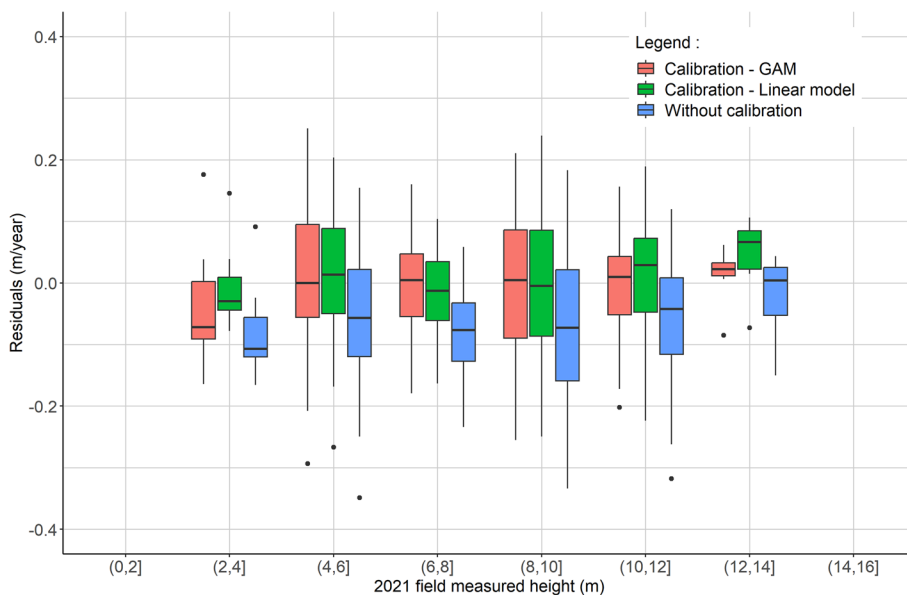


**Fig. 9** ALS height growth residuals according to 2021 field-measured height for the three calibrations (raw data, linear-calibrated, and GAM-calibrated). Height growth residual was calculated as ALS height growth – field-measured height growth

and precise descriptions of regenerating areas to prepare future wood resources in the context of global changes. These results could also support field operations, including tree-marking operations around considered regenerating areas, to optimize the spatial repartition of harvests for sapling height growth.

The method developed in this study also enables investigations of the regeneration state and dynamics in large-scale forest areas by allowing for the identification and mapping of regenerating areas, detection of dominant regeneration stems, and estimation of height and height growth. However, the proposed method does not provide data regarding the species that regenerate.

In forest inventories, data describing regeneration are typically collected in plots with low spatial and temporal resolutions while regeneration is a highly spatially heterogeneous component. This new method can therefore minimize the requirement of forest regeneration field inventories and improve their spatial coverage and the precision of the provided results. Inventory derived regeneration information is limited to presence-absence. The method developed herein opens new possibilities for describing forest regeneration.

The improvement of the spatial coverage and spatiotemporal resolution of regeneration data not only opens perspectives for silvicultural studies but also for

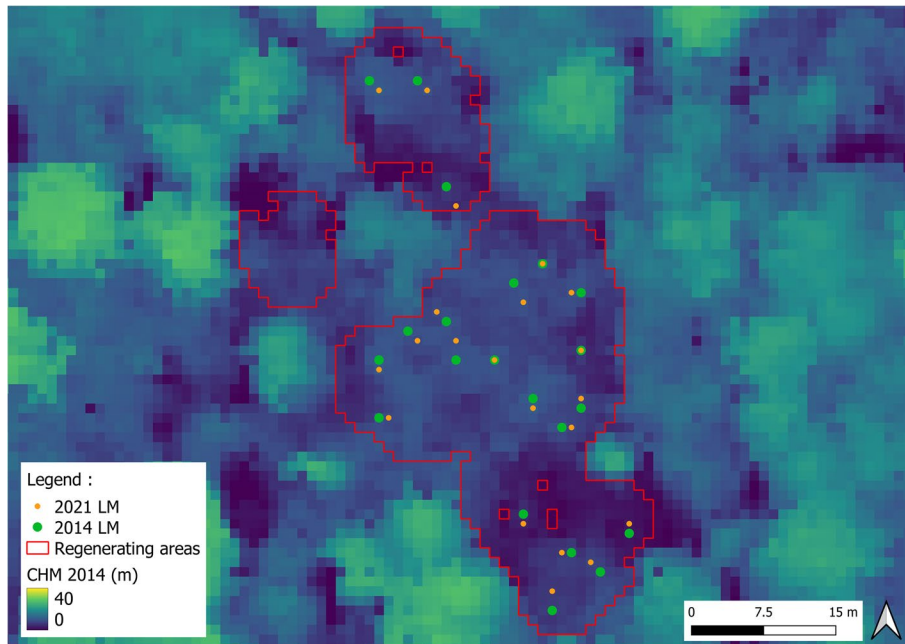


**Fig. 10** Example of regenerating areas (red) and matched local maxima (LM)

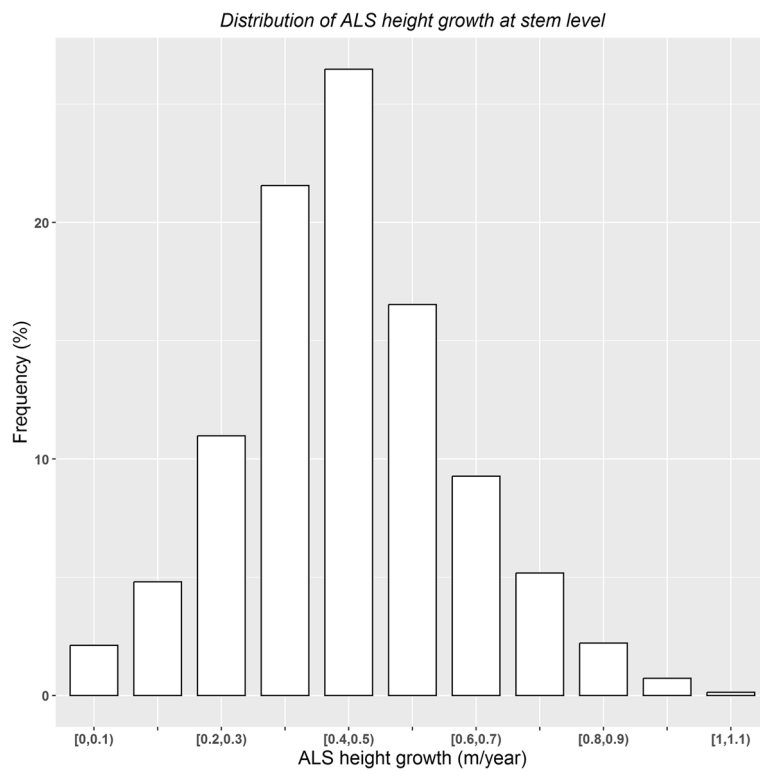


**Fig. 11** ALS height growth distribution at the stem level in the study area

fields not directly related to regeneration. For example, the movement ecology of wild ungulates requires habitat characterization across areas concordant with the target species' home ranges. Such studies are usually based on rough or punctual information (Allen et al. 2014; Licoppe 2006).

## 5 Conclusions

We developed a method to estimate the height and height growth of regeneration stems in forest gaps of a temperate uneven-aged deciduous forest using bi-temporal ALS data. This method considered differences in the two ALS acquisitions specifically calibrated by field data and the use of non-linear modeling, which improved ALS-estimated height for small regeneration stems. Regeneration height was estimated accurately while the proposed method produced unbiased height growth estimates (bias =  $-0.01 \text{ m}\cdot\text{year}^{-1}$ , RMSE =  $0.1 \text{ m}\cdot\text{year}^{-1}$ ). A total of 268,983 stems were detected throughout the study area, which had a mean height growth of 0.45 m/year.

Our results illustrated that estimating height and height growth of very young trees over large-scale areas is possible using bi-temporal ALS datasets. Such method has a great potential for forest management. The findings of this study will help to improve forest regeneration data collection.

### Abbreviations

ALS	Airborne laser scanning
CHM	Canopy height model
DBH	Diameter at breast height
GAM	Generalized additive model
LM	Local maxima
RMSE	Root-mean-squared error

### Acknowledgements

The authors thank the Public Service of Wallonia (SPW) for ALS sharing; Borremans A., Geerts C., Lemaigre B., and Reginster F. for field data collection; and the Department of Nature and Forests management—SPW, in particular the Florenville, Saint-Hubert, and Neufchâteau Sections, for their collaboration during field surveys.

### Authors' contributions

Conceptualization: LL, PL, and NL; methodology: LL, PL, and NL; software: LL; formal analysis and investigation: LL; validation: LL; resources: LL; data curation: LL; writing—original draft preparation: LL; writing—review and editing: NL, PL, RC, and GL; funding acquisition: PL; supervision: PL. The authors read and approved the final manuscript.

### Funding

This research was funded by the Walloon Region Forest Administration—CARTOFOR project, which is part of a 5-year forest research and training plan (2019–2024) and by University of Liège.

### Availability of data and materials

The datasets generated and analyzed during the current study are available on demand from the corresponding author.

### Code availability

The code is available on demand from the corresponding author.

## Declarations

### Ethics approval and consent to participate

Not applicable.

### Consent for publication

All authors gave their informed consent to this publication and its content.

### Competing interests

The authors declare that they have no conflict of interest. The funders had no role in the design of the study; in the collection, analyses, or interpretation of data; in the writing of the manuscript; or in the decision to publish the results.

### Author details

<sup>1</sup>TERRA Teaching and Research Centre—Forest Is Life, University of Liège (Liège)—Gembloux Agro-Bio Tech, Gembloux 5030, Belgium.

Received: 6 December 2023 Accepted: 20 August 2024

Published online: 26 September 2024

## References

- Alderweireld M, Burnay F, Pitchugin M, Lecomte H (2015) Inventaire forestier wallon-Résultats 1994 - 2012. Bilans et perspectives-Ressources naturelles SPW, DGO3, DNF, Direction des Ressources forestières, Jambes, Belgique. <https://hdl.handle.net/2268/181169>
- Allen AM, Månsson J, Jarnemo A, Bunnefeld N (2014) The impacts of landscape structure on the winter movements and habitat selection of female red deer. *Eur J Wildl Res* 60:411–421. <https://doi.org/10.1007/s10344-014-0797-0>
- Bolyn C, Lejeune P, Michez A, Latte N (2022) Mapping tree species proportions from satellite imagery using spectral-spatial deep learning. *Remote Sens Environ* 280:113205. <https://doi.org/10.1016/j.rse.2022.113205>
- Bosela M, Tumajer J, Cienciala E, Dobor L, Kulla L, Marčíš P, Popa I, Sedmák R, Sedmáková D, Sitko R, Šebeň V, Štěpánek P, Büntgen U (2021) Climate warming induced synchronous growth decline in Norway spruce populations across biogeographical gradients since 2000. *Sci Total Environ* 752:141794. <https://doi.org/10.1016/j.scitotenv.2020.141794>
- Candaele R, Ligot G, Licoppe A, Lievens J, Fichetef V, Jonard M, Lejeune P (2023) Interspecific growth reductions caused by wild ungulates on tree seedlings and their implications for temperate quercus-fagus forests. *Forests* 14:1330. <https://doi.org/10.3390/f14071330>
- Dupré S, Thiébaud B, Teissier Du Cros E (1985) Polycyclisme, vigueur et forme chez de jeunes hêtres plantés (*Fagus sylvatica* L.). *Revue forestière française* 37:6 456–464
- Feldmann E, Glatthorn J, Ammer C, Leuschner C (2020) Regeneration dynamics following the formation of understory gaps in a Slovakian beech virgin forest. *Forests* 11(5):585. <https://doi.org/10.3390/f11050585>
- Heurich M, Persson A, Holmgren J, Kennel E (2003) Detecting and measuring individual trees with laser scanning in mixed mountain forest of central Europe using an algorithm developed for Swedish boreal forest conditions. *Int Arch Photogramm Remote Sens Spat Inf Sci* 36(Part 8):W2
- Holmgren J, Nilsson M (2003) Estimation of tree height and stem volume on plots using airborne laser scanning. *Forest Science* 49:419–428. <https://doi.org/10.1093/forestscience/49.3.419>
- Hopkinson C, Chasmer L, Hall RJ (2008) The uncertainty in conifer plantation growth prediction from multi-temporal lidar datasets. *Remote Sens Environ* 112(3):1168–1180. <https://doi.org/10.1016/j.rse.2007.07.020>
- Illés G, Móczis N (2022) Climate envelope analyses suggests significant rearrangements in the distribution ranges of Central European tree species. *Ann for Sci* 79(1):1–19. <https://doi.org/10.1186/s13595-022-01154-8>
- Kangas A, Astrup R, Breidenbach J, Fridman J, Korhonen KT, Maltamo M, Nilsson M, Nord-T, Næsset E, Olsson H, Kangas A, Astrup R, Breidenbach J, Fridman J, Gobakken T, Korhonen KT, Maltamo M, Nilsson M, Nord-larsen T (2018) Remote sensing and forest inventories in Nordic countries - roadmap for the future. *Scand J for Res* 33(4):397–412. <https://doi.org/10.1080/02827581.2017.1416666>
- Khosravipour A, Skidmore AK, Isenburt M, Wang T, Hussin YA (2014) Generating pit-free canopy height models from airborne lidar. *Photogrammetric*

- Engineering & Remote Sensing 80:9 863–872. <https://doi.org/10.14358/PERS.80.9.863>
- Kiss S, Claessens H (2002) Les jeunes peuplements mélangés de hêtres et de bouleaux (étude bibliographique sur la forme des hêtres). *Forêt Wallonne* 55–56:2–14
- Leclère L, Latte N, Bolyn C, Lejeune P (2021) Mapping natural regeneration in canopy gaps from seedlings to saplings in uneven-aged deciduous forests using ALS data. *Proceedings of the SilviLaser Conference 2021*:28–30. <https://doi.org/10.34726/wim.1923>
- Leclère L, Lejeune P, Bolyn C, Latte N (2022) Estimating species-specific stem size distributions of uneven-aged mixed deciduous forests using ALS data and neural networks. *Remote Sensing* 14(6):1362. <https://doi.org/10.3390/rs14061362>
- Licoppe AM (2006) The diurnal habitat used by red deer (*Cervus elaphus* L.) in the Haute Ardenne. *European Journal of Wildlife Research* 52:3 164–170. <https://doi.org/10.1007/s10344-006-0027-5>
- Ligot G, Balandier P, Fayolle A, Lejeune P, Claessens H (2013) Height competition between *Quercus petraea* and *Fagus sylvatica* natural regeneration in mixed and uneven-aged stands. *For Ecol Manage* 304:391–398. <https://doi.org/10.1016/j.foreco.2013.05.050>
- Ma Q, Su Y, Tao S, Guo Q (2018) Quantifying individual tree growth and tree competition using bi-temporal airborne laser scanning data: a case study in the Sierra Nevada Mountains. *California International Journal of Digital Earth* 11(5):485–503. <https://doi.org/10.1080/17538947.2017.1336578>
- Maltamo M, Naesset E, Vauhkonen J (2014) Forestry applications of airborne laser scanning – concepts and case studies. *Managing Forest Ecosystems* 27:460p
- Maltamo M, Packalen P, Kangas A (2020) From comprehensive field inventories to remotely sensed wall-to-wall stand attribute data—a brief history of management inventories in the Nordic countries. *Can J for Res* 51:257–266. <https://doi.org/10.1139/cjfr-2020-0322>
- Martinez del Castillo E, Zang CS, Buras A, Hackett-Pain A, Esper J, Serrano-Nottivoli R, Hartl C, Weigel R, Klesse S, Resco de Dios V, Scharnweber T, Dorado-Liñán I, van der Maaten-Theunissen M, van der Maaten E, Jump A, Mikac S, Banzragch BE, Beck W, Cavin L, Claessens H, Čada V, Čufar K, Dulamsuren C, Gričar J, Gil-Pelegrín E, Janda P, Kazimirovic M, Kreyling J, Latte N, Leuschner C, Longares LA, Menzel A, Merela M, Motta R, Muffler L, Nola P, Petritan AM, Petritan IC, Prislán P, Rubio-Cuadrado Á, Rydval M, Stajić B, Svoboda M, Toromani E, Trotsiuk V, Wilmking M, Zlatanov T, de Luis M (2022) Climate-change-driven growth decline of European beech forests. *Communication Biology* 5(1):1–9. <https://doi.org/10.1038/s42003-022-03107-3>
- Michez A, Huylenbroeck L, Bolyn C, Latte N, Bauwens S, Lejeune P (2020) Can regional aerial images from orthophoto surveys produce high quality photogrammetric canopy height model? A single tree approach in Western Europe. *Int J Appl Earth Obs Geoinf* 92:102190. <https://doi.org/10.1016/j.jag.2020.102190>
- Næsset E, Gobakken T (2005) Estimating forest growth using canopy metrics derived from airborne laser scanner data. *Remote Sens Environ* 96(3):453–465. <https://doi.org/10.1016/j.rse.2005.04.001>
- Noyer E, Ningre F, Dlouhá J, Fournier M, Collet C (2019) Time shifts in height and diameter growth allocation in understory European beech (*Fagus sylvatica* L.) following canopy release. *Trees* 33:333–344. <https://doi.org/10.1007/s00468-018-1779-8>
- Petritan AM, von Lüpke B, Petritan IC (2009) Influence of light availability on growth, leaf morphology and plant architecture of beech (*Fagus sylvatica* L.), maple (*Acer pseudoplatanus* L.) and ash (*Fraxinus excelsior* L.) saplings. *Eur J Forest Res* 128:61–74. <https://doi.org/10.1007/s10342-008-0239-1>
- Pommerening A, Murphy ST (2004) A review of the history, definitions and methods of continuous cover forestry with special attention to afforestation and restocking. *Forestry* 77(1):27–44. <https://doi.org/10.1093/forestry/77.1.27>
- Popescu SC, Wynne RH (2004) Seeing the trees in the forest: using lidar and multispectral data fusion with local filtering and variable window size for estimating tree height. *Photogrammetric Engineering & Remote Sensing* 70:5 589–604. <https://doi.org/10.14358/PERS.70.5.589>
- R Core Team (2020). R: a language and environment for statistical computing. R Foundation for Statistical Computing, Vienna, Austria. <https://www.R-project.org/>
- Ramirez JI, Jansen PA, Poorter L (2018) Effects of wild ungulates on the regeneration, structure and functioning of temperate forests: a semi-quantitative review. *For Ecol Manage* 424:406–419. <https://doi.org/10.1016/j.foreco.2018.05.016>
- Roussel JR, Caspersen J, Béland M, Thomas S, Achim A (2017) Removing bias from LiDAR-based estimates of canopy height: Accounting for the effects of pulse density and footprint size. *Remote Sens Environ* 198:1–16. <https://doi.org/10.1016/j.rse.2017.05.032>
- Roussel JR, Auty D, Coops NC, Tompalski P, Goodbody TRH, Meador AS, Bourdon JF, de Boissieu F, Achim A (2020) lidR: an R package for analysis of airborne laser scanning (ALS) data. *Remote Sens Environ* 251:112061. <https://doi.org/10.1016/j.rse.2020.112061>
- Sénécal S, Brice K, Sauban F, Duvauchelle M, Morin A, Rombaut G, Bouan G, Couette A, Blondet M, Lenglet J, Wernsdörfer H (2020) La crise des scolytes (*Ips typographus*) ravageurs de l'Épicéa commun (*Picea abies*) vue de l'intérieur Retours sur une enquête qualitative auprès d'acteurs du nord-est de la France et sa zone transfrontalière (Allemagne, Belgique) réalisée fin 2019 - début. *Revue forestière française* 72:5 425–441. <https://doi.org/10.20870/revforfr.2020.5337>
- Song Y, Imanishi J, Sasaki T, Ioki K, Morimoto Y (2016) Estimation of broad-leaved canopy growth in the urban forested area using multi-temporal airborne LiDAR datasets. *Urban Forestry & Urban Green* 16:142–149. <https://doi.org/10.1016/j.ufug.2016.02.007>
- Stancioiu PT, O'hara KL (2006) Regeneration growth in different light environments of mixed species, multiaged, mountainous forests of Romania. *Eur J Forest Res* 125:151–162. <https://doi.org/10.1007/s10342-005-0069-3>
- Teissier du Cros E (1981) Le hêtre. *Quae*
- Thiébaud B, Comps B, Rucart M, Soroste S, Ntsame Okwo C (1992) Développement des plants de hêtre (*Fagus sylvatica* L.) dans une régénération naturelle, équienne, âgée de 18 ans. *Ann for Sci* 49(2):111–131
- Vepakomma U, St-Onge B, Kneeshaw D (2008) Height growth of regeneration in boreal forest canopy gaps - does the type of gap matter? An assessment with lidar time series. In: *SilviLaser 2008*. Edinburgh, p 9
- Vepakomma U, Kneeshaw D, St-Onge B (2010) Interactions of multiple disturbances in shaping boreal forest dynamics: a spatially explicit analysis using multi-temporal lidar data and high-resolution imagery. *J Ecol* 98(3):526–539. <https://doi.org/10.1111/j.1365-2745.2010.01643.x>
- Vepakomma U, St-Onge B, Kneeshaw D (2011) Response of a boreal forest to canopy opening: assessing vertical and lateral tree growth with multi-temporal lidar data. *Ecological Application* 21(1):99–121. <https://doi.org/10.1890/09-0896.1>
- Vidal C, Alberti I, Hernandez L, Redmond J (2016) National forest inventories, vol 10. Springer Science+ Business Media, Cham, pp 978–3
- Wang Y, Lehtomäki M, Liang X, Pyörälä J, Kukko A, Jaakkola A, Liu J, Feng Z, Chen R, Hyypää J (2019) Is field-measured tree height as reliable as believed - a comparison study of tree height estimates from field measurement, airborne laser scanning and terrestrial laser scanning in a boreal forest. *ISPRS J Photogramm Remote Sens* 147:132–145. <https://doi.org/10.1016/j.isprsjprs.2018.11.008>
- Wood SN (2017) Generalized additive models: an introduction with R, second edition. 496 p. <https://doi.org/10.1201/9781315370279>
- Yu X, Hyypää J, Kaartinen H, Maltamo M (2004) Automatic detection of harvested trees and determination of forest growth using airborne laser scanning. *Remote Sens Environ* 90(4):451–462. <https://doi.org/10.1016/j.rse.2004.02.001>
- Yu X, Hyypää J, Kukko A, Maltamo M, Kaartinen H (2006) Change detection techniques for canopy height growth measurements using airborne laser scanner data. *Photogrammetry and Remote Sensing* 72:12 1339–1348. <https://doi.org/10.14358/PERS.72.12.1339>
- Zhao K, Suarez JC, Garcia M, Hu T, Wang C, Londo A (2018) Utility of multi-temporal lidar for forest and carbon monitoring: tree growth, biomass dynamics, and carbon flux. *Remote Sens Environ* 204:883–897. <https://doi.org/10.1016/j.rse.2017.09.007>

## Publisher's Note

Springer Nature remains neutral with regard to jurisdictional claims in published maps and institutional affiliations.